Chemical Engineering Journal 154 (2009) 267–273

Contents lists available at ScienceDirect

Chemical Engineering Journal

journal homepage: www.elsevier.com/locate/cej

Ethanol steam reforming and water gas shift reaction over Co–Mn/ZnO catalysts

Albert Casanovas [a], Carla de Leitenburg [b], Alessandro Trovarelli [b], Jordi Llorca [a,*]

[a] Institut de Tècniques Energètiques, Universitat Politècnica de Catalunya, Av. Diagonal 647, Ed. ETSEIB, 08028 Barcelona, Spain
[b] Dipartimento de Scienze e Tecnologie Chimiche, Università di Udine, via del Cotonificio 108, 33100 Udine, Italy

ARTICLE INFO

Article history:
Received 3 December 2008
Received in revised form 19 January 2009
Accepted 19 January 2009

Keywords:
Ethanol steam reforming
Water gas shift
Hydrogen
Catalytic monolith
Cobalt catalyst
Co–Mn catalyst

ABSTRACT

The promotion effect of Mn over Co/ZnO catalysts in the steam reforming of ethanol (ESR) and water gas shift (WGS) has been studied in samples prepared by impregnation or co-precipitation with Mn_{at}/Co_{at} = 0.05–0.35. Alloy particles in Co–Mn/ZnO catalysts prepared by impregnation are smaller as deduced from high resolution transmission electron microscopy (HRTEM) and exhibit a rapid and higher degree of redox exchange between reduced and oxidized Co as deduced from temperature programmed reduction (TPR) and oxidation pulse experiments with respect to Co–Mn catalysts prepared by co-precipitation, which show a stronger Mn segregation on the surface, as deduced from X-ray photoelectron spectroscopy (XPS). Honeycomb catalysts have been prepared with the best catalytic formulation, a sample prepared by impregnation with $Mn_{at}/Co_{at} \sim 0.1$ and 10 wt.% Co, and tested in ESR and WGS as well. Honeycombs show good adherence of catalyst coatings and are significantly more active and selective than Co/ZnO honeycomb samples in both reactions.

1. Introduction

The search for an active and selective catalyst for the generation of hydrogen through ethanol steam reforming (1) at low temperature constitutes an active research area since ethanol is a renewable fuel (a bioethanol-to-H_2 system has the advantage of being CO_2 neutral) with low toxicity and high energy density that is also easy to handle and distribute [1–3].

$$C_2H_5OH + 3H_2O \rightarrow 6H_2 + 2CO_2 \quad (1)$$

There are numerous studies that demonstrate the feasibility of generating hydrogen from ethanol–water mixtures through catalytic steam reforming, either with powder catalysts [4,5] and with catalytic walls [6–9]. Among all catalysts tested so far, those based on cobalt exhibit the highest activity and selectivity towards hydrogen at low temperature [10–26]. Concerning the support, acidic supports should be avoided since they favor ethanol dehydration into ethylene, which is precursor of coke, whereas supports with both basic and redox characteristics are preferred, such as ZnO [27]. Thus, much work has been carried out over the Co/ZnO system. It has been demonstrated by *in situ* magnetic studies coupled to reaction tests and by *in situ* diffuse reflectance infrared spectroscopy [28–30] under real operation that the simultaneous presence of metallic cobalt and cobalt oxide is required for the progress of the reaction. Two steps of the reaction have been identified. First, ethanol dehydrogenates into acetaldehyde and hydrogen (2) over cobalt oxide (Co_3O_4). Hydrogen partly reduces the surface of cobalt particles into metallic cobalt and then, the second step, the reforming of acetaldehyde into the final products H_2 and CO_2, takes place (3) with the participation of the water gas shift reaction (4).

$$C_2H_5OH \rightarrow CH_3CHO + H_2 \quad (2)$$

$$CH_3CHO + 3H_2O \rightarrow 5H_2 + 2CO_2 \quad (3)$$

$$H_2O + CO \leftrightarrow H_2 + CO_2 \quad (4)$$

In order to favor the redox exchange between metallic cobalt and cobalt oxide under reaction conditions, several cobalt alloy formulations have been attempted. Alloying cobalt with the more electronegative first-row transition metals Ni and Cu resulted in a poor performance for the ethanol steam reforming reaction, due to a strong cobalt electron donation that prevented extensive Co reduction under reaction [31]. Also, alloying cobalt with noble metals favors the formation of methane through ethanol decomposition. In contrast, alloying cobalt with the less electronegative first-row transition metals Fe and Mn showed to be positive for the steam reforming of ethanol in terms of both catalytic activity and selectivity towards hydrogen [32]. In this work, two series of Co–Mn catalysts supported on ZnO with different Co:Mn ratios have been prepared by impregnation and co-precipitation methods and tested in the ethanol steam reforming and water gas shift reactions with the aim of unveil the role of the preparation method as well as identify the suitable Co:Mn ratio. Then, the best catalyst formulation has been used to prepare honeycomb catalysts useful for industrial environments or for mobile applications, such as fuel cell powered

* Corresponding author. Tel.: +34 93 401 17 08; fax: +34 93 401 71 49.
E-mail address: jordi.llorca@upc.edu (J. Llorca).

1385-8947/$ – see front matter © 2009 Elsevier B.V. All rights reserved.
doi:10.1016/j.cej.2009.01.024

vehicles equipped with internal reformers. Honeycomb catalysts have been also tested under ethanol steam reforming and water gas shift conditions.

2. Experimental

2.1. Preparation of powder catalysts

Two sets of Co–Mn/ZnO catalysts were prepared by impregnation and co-precipitation methods with a 10 wt.% Co content and Mn/Co = 0.05, 0.1, 0.2, and 0.35 molar ratios. For samples prepared by co-precipitation, a $(NH_4)_2CO_3$ solution (0.6 M) was added slowly to a mixture of $Zn(NO_3)_2$, $Co(NO_3)_2$, and $Mn(NO_3)_2$ aqueous solutions ($[M^{x+}] = 0.8$ M) at 303 K. After aging for 2 h the resulting solids were washed with distilled water, dried at 383 K overnight, and calcined in air at 673 K for 6 h. These catalysts were labeled as CoMn"*ac*", where "*a*" indicates the wt.% of Mn and "*c*" stands for "co-precipitation". For samples prepared by incipient wetness impregnation, an aqueous solution of $Co(NO_3)_2$, and $Mn(NO_3)_2$ was used over ZnO (Kadox 15). The solid was dried at 373 K overnight and calcined in air at 673 K for 6 h. These catalysts were labeled as CoMn"*ai*", where "*a*" indicates the wt.% of Mn and "*i*" stands for "impregnation". For comparative purposes, monometallic cobalt and manganese catalysts supported on ZnO, Co"*i*" and Mn"*i*", were prepared in a similar way.

2.2. Preparation of honeycomb catalysts

400 cpsi (cells per square inch) cordierite monolith cylinders with a diameter of 2 cm and a length of 2 cm were used. They were obtained by cutting larger monolith pieces with a diamond saw. Three types of honeycomb catalysts were prepared by the washcoating method from CoMn1i, Coi, and Mni vigorously agitated suspensions in de-ionized water (~5%, w/w). After each immersion monoliths were dried at 373 K under continuous rotation and then calcined at 673 K. This procedure was repeated several times in order to obtain the desired weight gain (10–12%, w/w). Honeycomb catalysts were labeled as WCoMn, WCo, and WMn ("W" stands for "washcoating").

2.3. Characterization

Mechanical stability of the catalyst coatings in honeycomb samples was evaluated by direct exposure to mechanical vibration. The vibration frequency was raised progressively from 20 to 50 Hz at a fixed acceleration value of 2 G, and at 50 Hz the acceleration was progressively increased from 2 to 10 G. Weight loss was monitored after 30 min at each frequency and acceleration, and after 3 h under the most severe vibration conditions (50 Hz, 10 G). G levels were controlled directly on the vibration test board with a Brüel & Kjaer 4370 accelerometer. Scanning electron microscopy was accomplished using a JEOL JSM 6400 instrument at an acceleration voltage of 20 kV. High resolution transmission electron microscopy (HRTEM) was conducted at 200 kV with a JEOL JEM 2010F microscope equipped with a field emission gun. Samples were dispersed in alcohol and deposited on grids with holey carbon films. For surface analysis, X-ray photoelectron spectroscopy (XPS) was performed with a Perkin-Elmer PHI-5500 instrument equipped with an Al X-ray source operated at 12.4 kV and a hemispherical electron analyzer. Surface area measurements (BET) were performed with a Micromeritics TriStar 3000 apparatus. Temperature programmed reduction (TPR) was carried out with a Micromeritics AutoChem II 2920 instrument using a H_2/Ar mixture (5% H_2) at 10 K min^{-1} and a TCD detector. Oxidation experiments were carried out at 723 K with 30 consecutive 0.05 mL oxygen pulses (1 pulse/min).

Table 1
Chemical composition and BET surface area of powder Co-Mn/ZnO catalysts.

Catalyst	% Co (w/w)	% Mn (w/w)	$m^2\ g^{-1}$
Prepared by impregnation			
Coi	9.3		10.2
Mni		9.9	10.7
CoMn0.5i	10.1	0.44	11.8
CoMn1i	10.1	1.0	9.9
CoMn2i	10.4	2.1	11.5
CoMn3i	9.6	3.5	11.5
Prepared by co-precipitation			
CoMn0.5c	10.1	0.45	23.6
CoMn1c	10.0	1.0	16.7
CoMn2c	10.1	2.0	19.5
CoMn3c	10.0	3.4	21.1

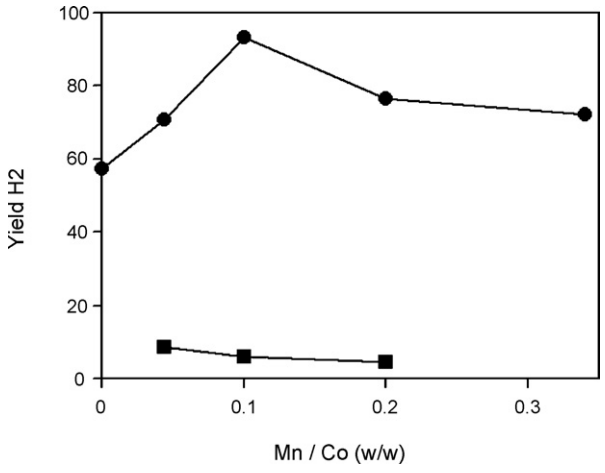

Fig. 1. Yield of hydrogen obtained under ethanol steam reforming of ethanol over Co–Mn/ZnO catalysts with different Mn/Co ratio prepared by impregnation (●) and co-precipitation (■). Reaction conditions: 623 K, atmospheric pressure, S/C = 3, 0.33 mL min^{-1} C_2H_5OH, GHSV = 10,000 h^{-1}.

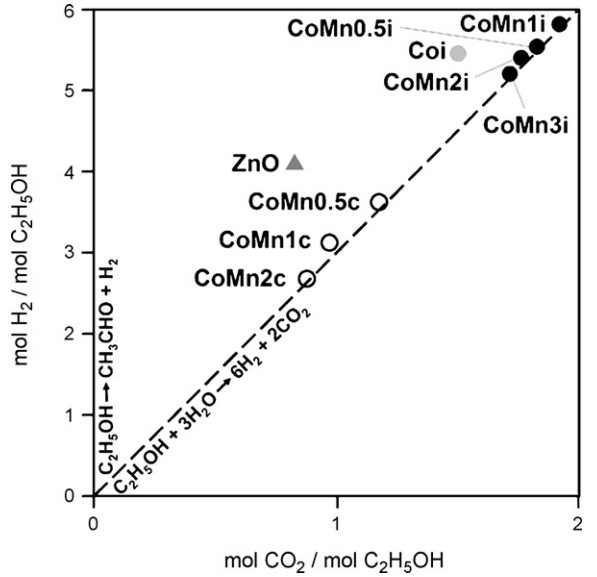

Fig. 2. Molar yield of H_2 and CO_2 with respect to ethanol introduced in the reaction mixture attained by monometallic Co/ZnO sample (●), bimetallic Co-Mn/ZnO catalysts prepared by impregnation (●), bimetallic Co–Mn/ZnO catalysts prepared by co-precipitation (○), and ZnO support (▲). Reaction conditions: 673 K, atmospheric pressure, S/C = 3, 0.33 mL min^{-1} C_2H_5OH, GHSV = 10,000 h^{-1}.

2.4. Catalytic tests

Ethanol steam reforming was carried out at atmospheric pressure and 473–773 K in a tubular reactor at a total flow of 80 mL min^{-1}. C_2H_5OH (0.33 mL min^{-1}) and H_2O were fed separately at a C_2H_5OH:H_2O molar ratio of 1:6 and the mixture was balanced with He. The effluent of the reactor was monitored on line with a MKS Cirrus mass spectrometer. H_2, CO, CO_2, CH_4, CH_3CHO, CH_3COCH_3, CH_3COOH, H_2O, and C_2H_5OH partial pressures were calibrated using appropriate standards and an Agilent micro-GC. Samples were first pretreated inside the reactor with a H_2:N_2 mixture (50 mL min^{-1}, 10% H_2) at 723 K for 4 h, the temperature was lowered to 473 K under N_2, and then the reaction mixture was introduced at 473 K. Monoliths operated under isothermal conditions as deduced from temperature monitoring inside their channels, located either in contact with the reactor wall or at the center of the reactor. The water gas shift reaction was carried out at atmospheric pressure in the 473–673 K temperature range using a CO:H_2:H_2O:N_2 = 1:2:6:14 molar mixture (total flow 50 mL min^{-1}). Water was provided with a syringe pump and vaporized before entering the reactant stream. Analysis of products was performed with a Varian micro-GC.

3. Results and discussion

3.1. Effect of Mn addition to Co/ZnO

Table 1 compiles the catalysts prepared along with their surface area (BET method) and chemical composition. Catalysts prepared by co-precipitation exhibited higher surface area values (about 20 m^2 g^{-1}) with respect to samples prepared by impregnation (ca. 10 m^2 g^{-1}). Fig. 1 shows the catalytic behavior of all samples in the ethanol steam reforming (17.7 g_{cat} min/mol C_2H_5OH) in terms of hydrogen yield at 623 K (defined as 100 mol $C_2H_5OH_{converted}$ mol H_2/mol $C_2H_5OH_{feed}$ mol products). It is evident that catalysts prepared by impregnation performed much better than those prepared by the co-precipitation method under the conditions tested. At this temperature, the yield of hydrogen is about 7–9 times higher for catalysts prepared by impregnation on a catalyst weight basis. On a surface area basis, the difference is about 15–20 times higher, meaning that the preparation method has a strong role in determining the catalytic behavior of Co–Mn/ZnO samples in the ethanol steam reforming. The catalytic performance follows the trend:

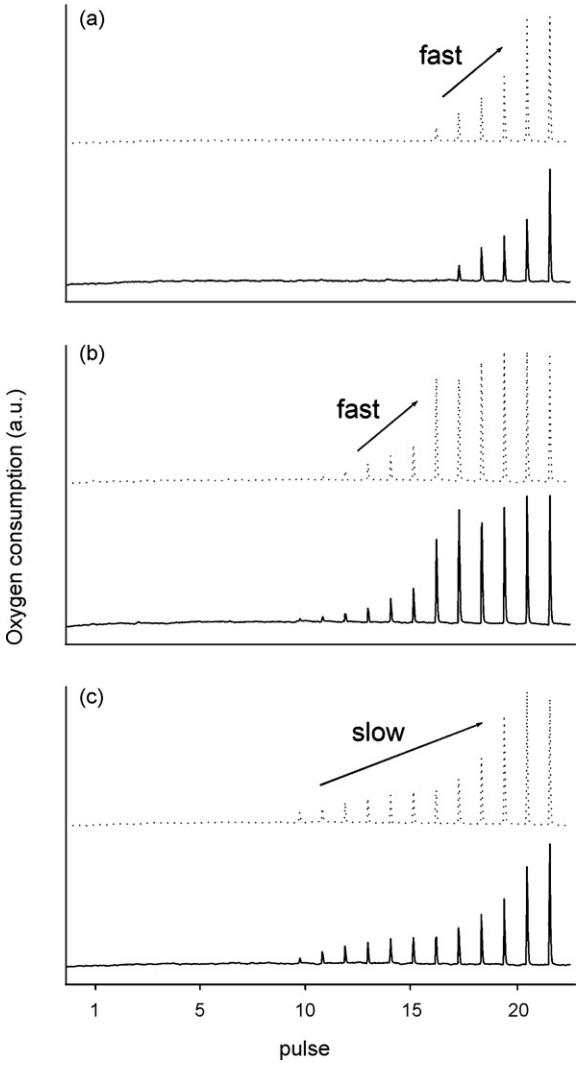

Fig. 3. Consumption of oxygen pulses of CoMn1i (a), CoMn1c (b), and Coi (c) samples after temperature programmed reduction experiment TPR1 (solid line) and TPR2 (dotted line).

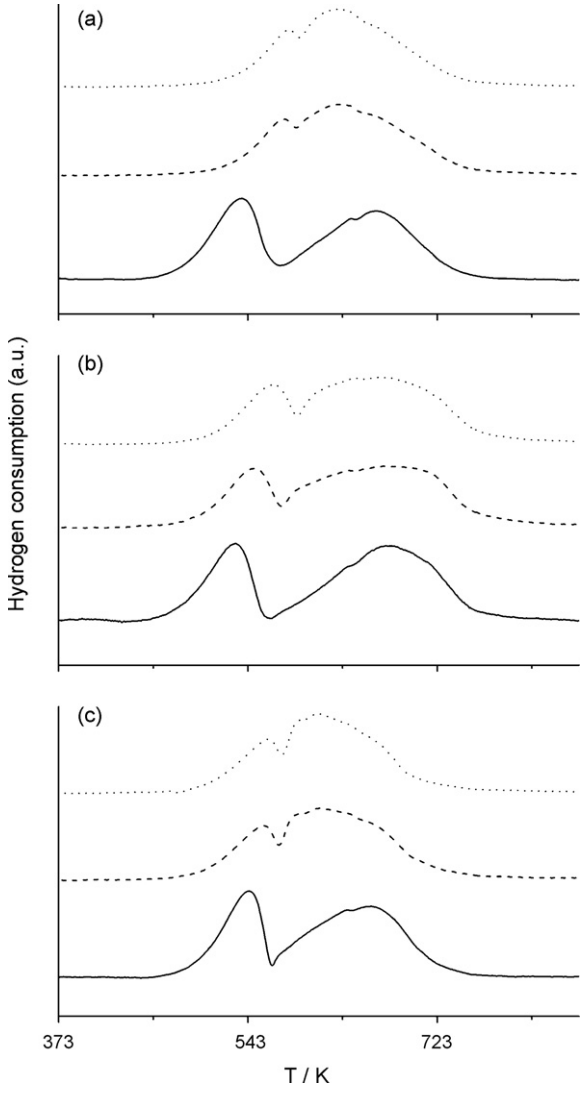

Fig. 4. Temperature programmed reduction profiles of catalysts CoMn1i (a), CoMn1c (b), and Coi (c) recorded over fresh samples (TPR1, solid line), and after oxygen pulse experiments (TPR2, dashed line; TPR3, dotted line).

CoMn1i > CoMn2i > CoMn3i > CoMn0.5i > Coi

≫ CoMn0.5c > CoMn1c > CoMn2c

Fig. 2 shows the results attained at 673 K in a two-dimensional plot, where the amount of hydrogen obtained on a molar basis with respect to ethanol in the reaction stream is plotted against the amount of carbon dioxide obtained on a molar basis with respect to ethanol in the reaction stream. From the stoichiometry of the steam reforming of ethanol (1), the expected molar ratio H_2/CO_2 is 3. This is indicated in the graph as a dashed line (the "reforming line"). Other competitive routes for ethanol transformation (ethanol decomposition, dehydration, etc.) result in deviations from the reforming line, making this type of graph very useful, since the position of the different catalysts serve as a measure of both their activity and selectivity to the reforming products H_2 and CO_2. The support, ZnO, and the sample containing only ZnO-supported cobalt, Coi, were active for ethanol transformation, but they plot to the left side of the reforming line, thus indicating that ethanol reforming was accompanied by ethanol dehydrogenation (2), originating $H_2/CO_2 > 3$. As expected, Coi was more active than ZnO [10]. The location of Co–Mn/ZnO samples in the graph strongly depended on the preparation method. Catalysts prepared by impregnation were much more active and selective for ethanol steam reforming than Coi and Co–Mn/ZnO samples prepared by co-precipitation. Interestingly, all Co–Mn/ZnO catalysts plot on the reforming line, irrespective of the preparation method, meaning that the addition of Mn has a strong positive effect on the selectivity of Co-based catalysts for the reforming of ethanol. Concerning the effect of the Co:Mn ratio, the optimum value for ethanol steam reforming activity was around Mn/Co = 0.1 for catalysts prepared by impregnation, whereas the progressive addition of Mn in the co-precipitated samples resulted in a poorer catalytic performance (Figs. 1 and 2). Impregnated samples were also more active for the water gas shift reaction, particularly around 573 K. At this temperature and GHSV = 15,000 h^{-1}, catalysts prepared by impregnation attained CO conversions of 54–84%, whereas over samples prepared by co-precipitation the conversion of CO was in the range 36–54%.

Given the different catalytic performance between samples prepared by impregnation and co-precipitation methods, detailed temperature programmed reduction and oxygen pulse experiments were carried out over CoMn1i, CoMn1c, and Coi samples in order to study the redox exchange between oxidized and reduced cobalt, which has been demonstrated to be the clue for ethanol steam reforming over Co-based catalysts [28–30]. In particular, three TPR profiles and two oxidation experiments using oxygen pulses (OP) were alternated: TPR1 → OP1 → TPR2 → OP2 → TPR3. In Fig. 3, the consumption of oxygen pulses for the different samples is shown. The amount of oxygen uptake recorded over the CoMn1i sample was significantly higher than that of samples CoMn1c and Coi for both OP1 and OP2 experiments. Taking into account the metal loading of the different samples (Table 1), the extent of reoxidation for catalyst CoMn1i was about 90%, whereas for CoMn1c and

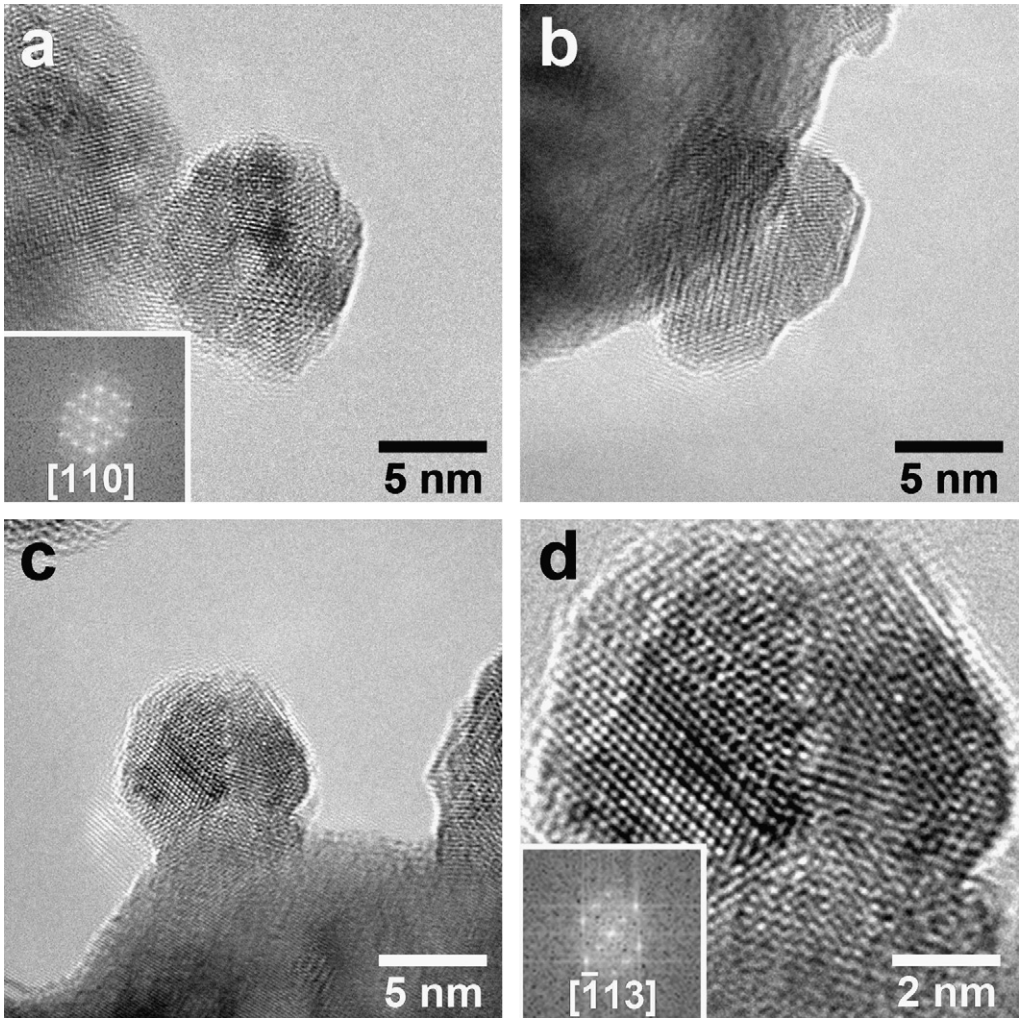

Fig. 5. Representative high resolution transmission electron microscopy images recorded over the CoMn1i catalyst.

Coi samples the degree of reoxidation was about 70%. In addition, the dynamics of the oxygen uptake differed considerably between bimetallic Co–Mn samples and monometallic Coi. In both CoMn1i and CoMn1c the transition between complete oxygen uptake and non-oxygen uptake was fast (4–5 pulses), whereas the transition in the Coi sample was significantly slower (9–10 pulses). Therefore, it can be concluded that the redox dynamics between oxidized and reduced cobalt is clearly enhanced in the presence of manganese, and that the redox exchange degree in the Co–Mn/ZnO catalyst prepared by impregnation is higher that of the sample prepared by co-precipitation. This may well account for the better catalytic performance of sample CoMn1i in the steam reforming of ethanol and water gas shift reaction. The temperature programmed reduction profiles recorded over these catalysts before and after each OP experiment are reported in Fig. 4. The temperature programmed reduction profiles recorded over the fresh samples, TPR1, showed in all cases two well-defined hydrogen uptake peaks centered at about 523–533 and 663–673 K, which correspond to the well known $Co_3O_4 \rightarrow CoO$ and $CoO \rightarrow Co$ transformations, respectively [8]. For the CoMn1i catalyst, however, the temperature programmed reduction profiles recorded after the oxygen pulse experiments, TPR2 and TPR3, strongly differed from the TPR1 profile since both hydrogen uptake signals occurred in a very narrow temperature interval, 573 and 638 K. In addition, an extra hydrogen uptake signal appeared at 623 K. This was also accompanied by a strong decrease in the low-temperature hydrogen uptake, meaning that the cobalt oxide formed upon oxidation is easily reduced, which again means that the redox exchange between oxidized and reduced cobalt is promoted by Mn in the sample prepared by impregnation. The effect is less pronounced for the CoMn1c sample. An accurate quantification of the oxygen and hydrogen uptakes in OP and TPR experiments indicates that the amount of cobalt that reversibly undergoes exchange between oxidized and reduced states in the CoMn1i sample is about 85%, whereas that in CoMn1c and Coi are about 65 and 60%, respectively.

In order to get further insight into the effect of the preparation method on the structural characteristics of Co–Mn/ZnO catalysts, HRTEM study was carried out over CoMn1i and CoMn1c samples after reduction. Fig. 5 shows several representative images of catalyst CoMn1i. Metal particles with a mean diameter of 8–12 nm were well-dispersed over ZnO. Lattice fringes, Fourier Transform images (insets in Fig. 5a and d), and EELS spectra revealed the formation of Co–Mn metallic alloy. In contrast, the CoMn1c sample was constituted by Co–Mn alloy metal particles with a mean diameter of 10–15 nm and covered by an oxide layer. This is well exemplified in Fig. 6, where particles exhibit in all cases a dark Co–Mn metallic core and a low-contrast oxide shell. The different redox dynamics between CoMn1i and CoMn1c could be originated by a particle size effect or/and by a more complex effect resulting from a different interaction between the particles and the support related to the preparation method. Another important parameter to take into account is the chemical composition of the surface of these two

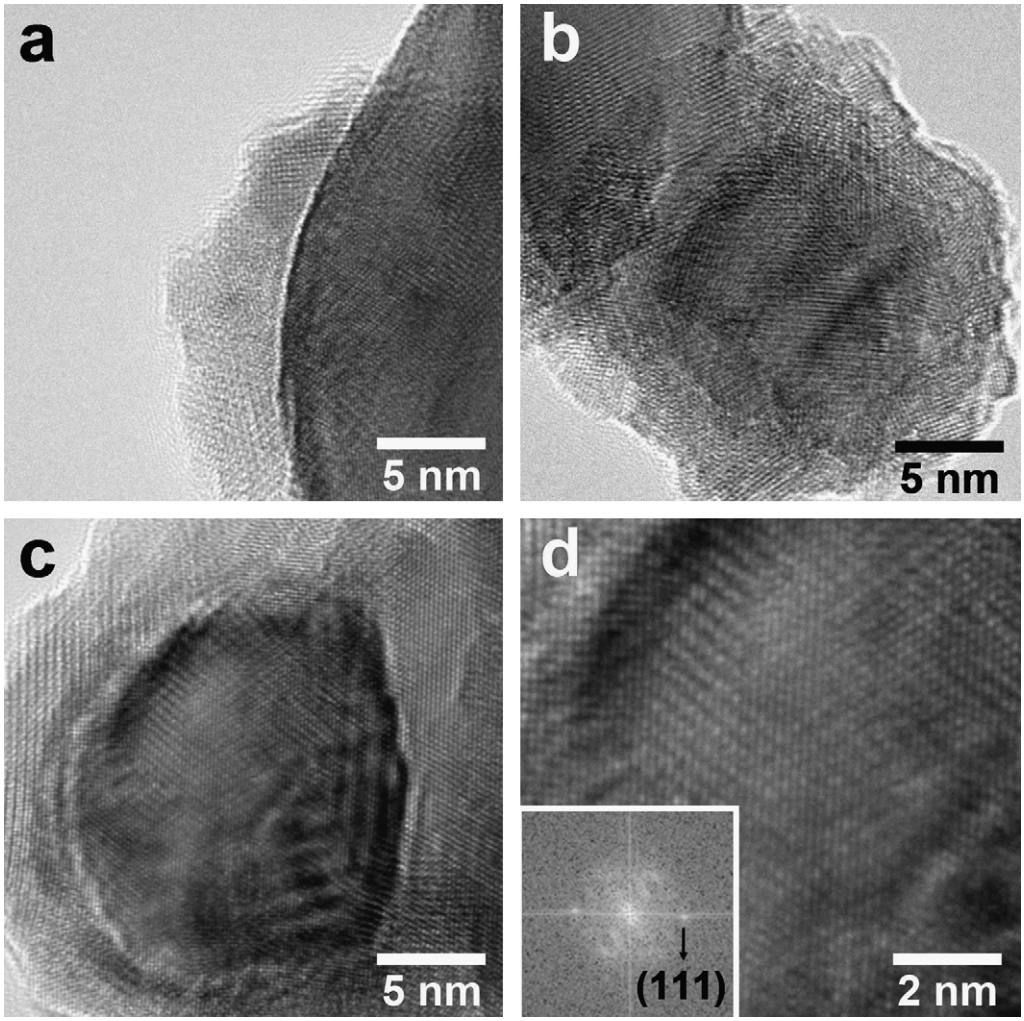

Fig. 6. Representative high resolution transmission electron microscopy images recorded over the CoMn1c catalyst.

catalysts. Although they contain the same metal loading (Table 1), XPS revealed a stronger segregation of Mn at the surface of the sample prepared by co-precipitation (Co/Mn = 2.29) than that of the impregnated catalyst (Co/Mn = 3.27). This could also influence the redox dynamics, which determines the catalytic performance.

3.2. Honeycomb catalysts

Honeycomb catalysts were prepared with the CoMn1i catalyst (WCoMn) since it exhibited the best catalytic performance for both ethanol steam reforming and water gas shift reaction. For comparison purposes, two other honeycomb samples were prepared containing only cobalt (WCo, prepared from Coi) or manganese (WMn, prepared from Mni). Catalytic honeycombs were imaged (SEM) in frontal and transverse views and a good catalyst coating homogeneity was observed in all cases. The mean catalytic layer thickness was about 200 μm. Mechanical stability of the catalytically active phase in honeycomb catalysts is a critical issue for practical application purposes because coating loss and banking up should be completely avoided. The weight loss of the catalytic coatings in honeycombs WCoMn and WCo was less than 4% after 5 h of exposure to mechanical vibration (up to 50 Hz and 10 G), which means an excellent adherence, whereas the weight loss of honeycomb WMn was considerably higher, about 30%.

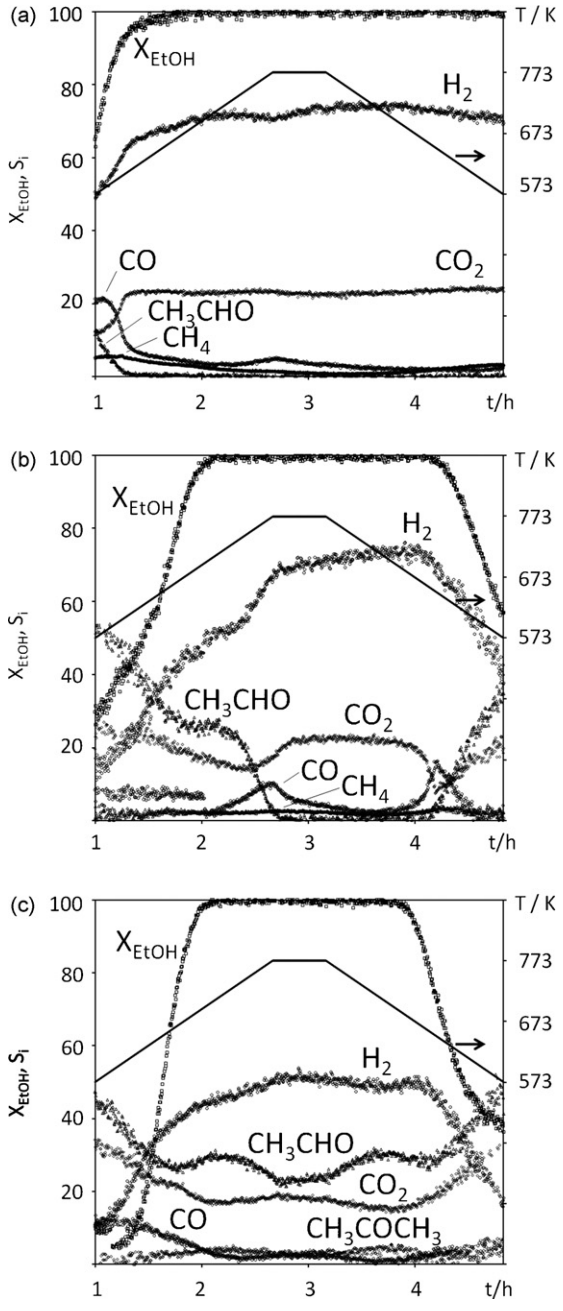

Fig. 7. Catalytic performance of honeycombs WCoMn (a), WCo (b), and WMn (c) in the ethanol steam reforming. S/C = 3, 0.33 mL C_2H_5OH min^{-1}, VHSV = 2500 h^{-1}.

The catalytic performance of honeycomb WCoMn for the steam reforming of ethanol is shown in Fig. 7a during a 573–773–573 K temperature cycle. Between 573 and about 623 K, ethanol transformed into a mixture of H_2, CO, CO_2, CH_3CHO, and CH_4, being $[CO]/[CO_2] \sim 1.7$ and $[CH_4]/[CO_2] \sim 0.44$. In this temperature region, various reactions occurred simultaneously. These are basically the ethanol dehydrogenation into acetaldehyde and hydrogen (2), the decomposition of ethanol into a mixture of H_2, CO, and CH_4, and the reforming of acetaldehyde (3). Above ca. 623 K, the transformation of ethanol was complete and the main products of the reaction were H_2 and CO_2. At this temperature, no more acetaldehyde was present as an intermediate product and the concentration of CH_4 decreased progressively $[CH_4]/[CO_2] \sim 0.08$, indicating that the decomposition route vanished and the reforming route was preferred. In addition, the amount of CO also decreased $[CO]/[CO_2] \sim 0.14$, due to water gas shift activity (4). At 723 K, the selectivity values of the reforming products were 71.5% H_2 and 23.0% CO_2, which correspond to an efficiency towards complete ethanol steam reforming of about 94%. At temperatures higher than ca. 743 K, the selectivity of H_2 and CO_2 decreased at the expense of CO due to the reverse gas shift reaction. Finally, when the temperature was decreased back to 573 K the catalytic performance was maintained due to the activation of the catalyst through Co reduction under steam reforming conditions [8,30].

These results strongly differ from the catalytic performance of honeycombs WCo and WMn. Fig. 7b shows the results attained for the ethanol steam reforming over honeycomb WCo. It is clear that the sample was less active and that at low temperature ethanol mainly dehydrogenated into acetaldehyde and H_2. Only at temperatures higher than 743 K a reactor effluent dominated by the reforming products, H_2 and CO_2, was obtained. However, at this temperature the reverse water gas shift reaction occurred and CO was obtained as well $[CO]/[CO_2] \sim 0.57$. In contrast to honeycomb WCoMn, when the temperature was lowered back to 573 K the activity of the honeycomb WCo was no longer maintained and acetaldehyde was again present among the reaction products. This can be explained in terms of different Co redox exchange facility in Co/ZnO and Co–Mn/ZnO samples as discussed in Section 3.1; the higher the redox exchange capacity, the easier the catalyst activation under steam reforming conditions. Under the same conditions, honeycomb WMn was even less active for ethanol steam reforming (Fig. 7c) and the yield towards hydrogen was the lowest because ethanol mainly dehydrogenated into acetaldehyde at all temperatures. In this case, a nearly symmetric pattern in ethanol conversion and product selectivity was obtained when the temperature was lowered back to 573 K due to absence of Co.

Honeycombs WCoMn and WCo were tested in the water gas shift reaction under conditions simulating the outlet of an ethanol steam reformer ($CO:H_2:H_2O = 1:2:6$). Table 2 shows the catalytic performance in terms of CO conversion and CH_4/CO_2 molar ratios obtained. Conversion of CO started at 523 K for WCoMn and 573 K for WCo, strongly suggesting that the low amount of CO obtained under ESR conditions was partly due to WGS activity of catalytic honeycombs. CO conversion over honeycomb WCoMn was always higher than that of sample WCo, especially at low temperature. This is also in accordance to the results reported above for the

Table 2
Catalytic performance of honeycomb catalysts in the water gas shift reaction. $CO:H_2:H_2O:N_2 = 1:2:6:14$, VHSV = 6000 h^{-1}.

T/K	CO conversion/%		CH_4/CO_2	
	WCoMn	WCo	WCoMn	WCo
523	0.9	0.3	–	–
573	28.1	1.8	0.022	–
623	64.1	59.7	0.010	0.005
673	90.5	84.3	0.006	0.003

ethanol steam reforming, where the CO concentration at the outlet of honeycomb WCoMn was much lower than that of sample WCo (Fig. 7). Under these conditions almost no methanation occurred (Table 2).

4. Conclusions

Mn-promoted Co/ZnO powder catalysts and honeycomb structures are effective for hydrogen production at low temperature from ethanol steam reforming and water gas shift reaction. The presence of Mn facilitates the redox exchange between reduced and oxidized Co, which has a positive effect on both reactions. The preparation method of the catalysts and the Mn/Co ratio play a crucial role in the catalytic performance. Samples prepared by incipient wetness impregnation contain Co–Mn alloy nanoparticles and exhibit excellent catalytic behavior, whereas samples prepared by co-precipitation exhibit a poor catalytic behavior and contain alloy particles covered by an oxide shell with Mn segregation on the surface. The best catalytic results for ethanol steam reforming have been obtained over a catalyst prepared by impregnation and containing 10 wt.% Co with Mn/Co = 0.1.

Acknowledgements

This work was supported by MEC grant ENE2006-06925. A.T. and C.d.L. thank regione Friuli Venezia Giulia and MIUR for financial support.

References

[1] G.A. Deluga, J.R. Salge, L.D. Schmidt, X.E. Verykios, Science 303 (2004) 993.
[2] F. Frusteri, S. Freni, J. Power Sources 173 (2007) 200.
[3] V.A. Kirillov, V.D. Meshcheryakov, V.A. Sobyanin, V.D. Belyaev, Y.I. Arnosov, N.A. Kuzin, A.S. Bobrin, Theor. Found. Chem. Eng. 42 (2008) 1.
[4] A. Haryanto, S. Fernando, N. Murali, S. Adhikari, Energy Fuels 19 (2005) 2098.
[5] P.D. Vaidya, A.E. Rodrigues, Chem. Eng. J. 117 (2006) 39.
[6] A. Casanovas, M. Saint-Gerons, F. Griffon, J. Llorca, Int. J. Hydrogen Energy 33 (2008) 1827.
[7] J. Llorca, A. Casanovas, T. Trifonov, A. Rodríguez, R. Alcubilla, J. Catal. 255 (2008) 228.
[8] A. Casanovas, C. De Leitenburg, A. Trovarelli, J. Llorca, Catal. Today 138 (2008) 187.
[9] M. Domínguez, E. Taboada, E. Molins, J. Llorca, Catal. Today 138 (2008) 193.
[10] J. Llorca, N. Homs, J. Sales, P. Ramírez de la Piscina, J. Catal. 209 (2002) 306.
[11] J. Llorca, P. Ramírez de la Piscina, J.A. Dalmon, J. Sales, N. Homs, Appl. Catal. B 43 (2003) 355.
[12] S. Tuti, F. Pepe, Catal. Lett. 122 (2008) 196.
[13] A.E. Galetti, M.F. Gomez, L.A. Arrua, A.J. Marchi, M.C. Abello, Catal. Commun. 9 (2008) 1201.
[14] J.C. Vargas, S. Libs, A.C. Roger, A. Kiennemann, Catal. Today 107 (2005) 417.
[15] J. Llorca, N. Homs, J. Sales, J.L.G. Fierro, P. Ramírez de la Piscina, J. Catal. 323 (2004) 470.
[16] P. Bichon, G. Haugom, H.J. Venvik, A. Colmen, E.A. Blekkan, Top. Catal. 49 (2008) 38–45.
[17] S.S.Y. Lin, D.H. Kim, S.Y. Ha, Catal. Lett. 122 (2008) 295–301.
[18] S. Freni, S. Cavallaro, N. Mondello, L. Spadaro, F. Frustreri, Catal. Commun. 4 (2003) 259.
[19] J. Sun, X.-P. Qiu, F. Wu, W.-T. Zhu, Int. J. Hydrogen Energy 30 (2005) 437.
[20] F. Mariño, G. Baronetti, M. Jobbagy, M. Laborde, Appl. Catal. A 238 (2003) 41.
[21] M.S. Batista, R.K.S. Santos, E.M. Assaf, J.M. Assaf, E.A. Ticianelli, J. Power Sources 134 (2004) 27.
[22] H. Song, L. Zhang, R.B. Watson, D. Braden, U.S. Ozkan, Catal. Today 129 (2007) 346.
[23] H. Wang, J.L. Ye, Y. Liu, Y.D. Li, Y.N. Qin, Catal. Today 129 (2007) 305.
[24] M. Benito, R. Padilla, L. Rodríguez, J.L. Sanz, L. Daza, J. Power Sources 169 (2007) 167.
[25] A. Kaddouri, C. Mazzocchia, Catal. Commun. 5 (2004) 339.
[26] F. Haga, T. Nakajima, H. Miya, S. Mishima, Catal. Lett. 48 (1997) 223.
[27] J. Llorca, P. Ramírez de la Piscina, J. Sales, N. Homs, Chem. Commun. (2001) 641.
[28] J. Llorca, J.A. Dalmon, P. Ramírez de la Piscina, N. Homs, Appl. Catal. A 243 (2003) 261.
[29] J. Llorca, N. Homs, P. Ramírez de la Piscina, J. Catal. 227 (2004) 556.
[30] J. Llorca, P. Ramírez de la Piscina, J.A. Dalmon, N. Homs, Chem. Mater. 16 (2004) 3573.
[31] N. Homs, J. Llorca, P. Ramírez de la Piscina, Catal. Today 116 (2006) 361–366.
[32] J.A. Torres, J. Llorca, A. Casanovas, M. Domínguez, J. Salvadó, D. Montané, J. Power Sources 169 (2007) 158.